Journal of Cellular Biochemistry 88:1273–1291 (2003)

Nuclear Trafficking of FGFR1: A Role for the Transmembrane Domain

Jason M. Myers, Gabriel G. Martins, Jacek Ostrowski, and Michal K. Stachowiak*

Molecular and Structural Neurobiology and Gene Therapy Program, Department of Pathology and Anatomical Sciences, State University of New York at Buffalo, Buffalo, New York

Abstract Several members of the fibroblast growth factor (FGF) family lack signal peptide (SP) sequences and are present only in trace amounts outside the cell. However, these proteins contain nuclear localization signals (NLS) and accumulate in the cell nucleus. Our studies have shown that full length FGF receptor 1 (FGFR1) accumulates within the nuclear interior in parallel with FGF-2. We tested the hypothesis that an atypical transmembrane domain (TM) plays a role in FGFR1 trafficking into the nuclear interior. With FGFR1 destined for constitutive fusion with the plasma membrane due to its SP, how the receptor may enter the nucleus is unclear. Sequence analysis identified that FGFR1 has an atypical TM containing short stretches of hydrophobic amino acids (a.a.) interrupted by polar a.a. The β-sheet is the predicted conformation of the FGFR1 TM, in contrast to the α-helical conformation of other single TM tyrosine kinase receptors, including FGFR4. Receptor trafficking in live cells was studied by confocal microscopy via C-terminal FGFR1 fusions to enhanced green fluorescent protein (EGFP) and confirmed by subcellular fractionation and Western immunoblotting. Nuclear entry of FGFR1–EGFP was independent of karyokinessis, and was observed in rapidly proliferating human TE671 cells, in slower proliferating glioma SF763 and post-mitotic bovine adrenal medullary cells (BAMC). In contrast, a chimeric FGFR1/R4-EGFP, where the TM of FGFR1 was replaced with that of FGFR4, was associated with membranes (golgi-ER, plasma, and nuclear), but was absent from the nucleus and cytosol. FGFR1Δ-EGFP mutants, with hydrophobic TM a.a. replaced with polar a.a., showed reduced association with membranes and increased cytosolic/nuclear accumulation with an increase in TM hydrophilicity. FGFR1(TM−)-EGFP (TM deleted), was detected in the golgi-ER vesicles, cytosol, and nuclear interior; thus demonstrating that the FGFR1 TM does not function as a NLS. To test whether cytosolic FGFR1 provides a source of nuclear FGFR1, cells were transfected with FGFR1(SP−) (SP was deleted), resulting in cytosolic, non-membrane, protein accumulation in the cytosol and the cell nucleus. Our results indicate that an unstable association with cellular membranes is responsible for the release of FGFR1 into the cytosol and cytosolic FGFR1 constitutes the source of the nuclear receptor. J. Cell. Biochem. 88: 1273–1291, 2003.

Key words: FGF receptor; nuclear trafficking; transmembrane domain

Fibroblast growth factors (FGF) are signaling peptides that regulate cell survival, apoptosis, proliferation, differentiation, matrix composition, chemotaxis, cell adhesion, migration, and growth of cell processes [Stachowiak et al., 1997b; Szebeneyi and Fallon, 1999]. Classically, FGFs exert their biological effects in an autocrine or paracrine fashion, whereby they interact with transmembrane tyrosine kinase FGF receptors (FGFR) and promote their dimerization and activation [Szebeneyi and Fallon, 1999]. Several members of the FGF family, including FGF-2 and FGF-1, lack signal peptide (SP) sequences and are absent or are found in trace amounts outside the cell. Some of these proteins contain nuclear localization signals (NLS) (e.g., HMW isoforms-FGF-2) and are highly concentrated in the cell nucleus [Renko et al., 1990; Florkiewicz et al., 1991; Stachowiak et al., 1994, 1997b; Moffett et al., 1996; Joy et al., 1997].

Bovine adrenal medullary cells (BAMC), human astrocytes, and glioma cells contain high-affinity FGF-2 binding sites in the nucleus and on the cell surface, which represent FGFR1 [Stachowiak et al., 1996a,b, 1997b]. Hormonal,

Grant sponsor: NSF; Grant number: IBN-9728923; Grant sponsor: NIH; Grant numbers: HL-49376, NS43621-01.

*Correspondence to: Dr. Michal K. Stachowiak, Molecular and Structural Neurobiology and Gene Therapy Program, Department of Pathology and Anatomical Sciences, 317 Farber Hall, State University of New York at Buffalo, Buffalo, NY 14214. E-mail: mks4@buffalo.edu

Received 25 October 2002; Accepted 22 November 2002

DOI 10.1002/jcb.10476

neurotransmitter, or growth factor stimulation of these cells results in the rapid nuclear accumulation of FGF-2 and FGFR1, demonstrated by Western analysis of subcellular fractions and binding of ^{125}I-FGF-2. Intranuclear localization of FGFR1 was also shown by immunocytochemistry, and confocal and electron microscopy [Stachowiak et al., 1996a,b, 1997a; Peng et al., 2001, 2002]. Nuclear FGFR1 is full length, has FGF-regulated kinase activity, and undergoes autophosphorylation. The three FGFR1 isoforms (95, 105, and 130 kDa) observed on Western blots represent different degrees of FGFR1 glycosylation, shown by reduction to a single 95 kDa protein by treatment with *N*-glycanase [Stachowiak et al., 1997b]. Our findings are supported by studies in other laboratories, which showed localization of FGFR1 in the nuclei of neurons [Gonzales et al., 1995; Klimaschewski et al., 1999], fibroblasts [Maher, 1996; Reilly and Maher, 2001], and retinal cells [Guillonneau et al., 1998].

Nuclear accumulation of FGFR1 (which lacks a NLS) coincides with that of FGF-2 and was proposed to be chaperoned to the nucleus by HMW-FGF-2 [Stachowiak et al., 1996a; Peng et al., 2001, 2002] in β-importin-dependent manner [Reilly and Maher, 2001].

Although incubation of fibroblasts with exogenous 18 kDa FGF-2 resulted in the nuclear translocation of FGFR1 [Maher, 1996], in glioma, BAMC, or medulloblastoma TE671 cells, nuclear accumulation of FGFR1 could not be induced by extracellular FGF-2, but was elicited by unrelated growth factors, hormones, and stimulation of cAMP and Ca^{++} 2nd messengers. All stimuli that induce nuclear accumulation of FGFR1 also cause nuclear accumulation of non-released HMW FGF-2 [Stachowiak et al., 1994, 1996a,b; Peng et al., 2002]. Also, incubation of glioma or TE671 medulloblastoma cells with NHS-sulfobiotin did not lead to an appearance of biotinylated receptor in the nucleus [Stachowiak et al., 1997b; Peng et al., 2002], indicating that nuclear FGFR1 was not derived from the cell surface. However, it was also evident that nuclear FGFR1 is processed at least partially through the ER-golgi, indicated by its glycosylation. We hypothesized that the association of FGFR1 with the ER membranes may not be stable, and that the receptor is released into the cytosol before the endoplasmic vesicles fuse with the plasma membrane.

FGFR1 contains an N-terminal hydrophobic SP (amino acids, a.a. 2–20) [Hou et al., 1991]. A signal-recognition particle (SRP) binds to the SP as it emerges from the ribosome [Walter and Johnson, 1994; Stroud and Walter, 1999]. The SRP–ribosome complex binds to the SRP receptor exposed on the cytosolic surface of the rough ER. With the SP remaining bound near the pore proteins, the polypeptide elongates and translocates into the ER lumen via an aqueous pore. Upon reaching the hydrophobic transmembrane domain (TM) (stop-transfer peptide), the translated protein dissociates from the translocase and the hydrophobic TM stays anchored in the lipid bilayer [Walter and Johnson, 1994; Stroud and Walter, 1999]. When the SP is cleaved by the signal peptidase, the result is a TM protein with its N-terminal in the ER lumen and its C-terminal in the cytosol.

Typically, the TM is an α-helix of approximately 30 a.a. with >11 consecutive hydrophobic a.a. These non-polar a.a. are oriented outside the α-helical core and interact with the lipid bilayer thereby conferring stability to the peptide in the membrane [Creighton, 1984]. Disruption of this hydrophobic region by polar a.a. makes the protein association with membrane less stable [Eisenberg et al., 1984].

Studies in different laboratories have uncovered a novel mechanism through which proteins that are inserted into the endoplasmic reticulum (ER) membrane or are entirely within the ER lumen (secreted proteins) can be exported back to the cytosol [Romisch, 1999]. They showed that a protein-conducting channel formed by the Sec61 complex is responsible for both forward (insertion) and retrograde (removal) of proteins across the ER membrane. The retrograde transport machinery is coupled with the 26S proteasome complex [Immamura et al., 1998; Mayer et al., 1998]. Consequently, the retrieved transmembrane proteins may be degraded in the cytosol. However, it is possible that some proteins, including FGFR1, may escape degradation and function outside the ER.

MATERIALS AND METHODS

Cell Culture

Human SF763-glioma, TE671 medulloblastoma cell lines and primary cultures of BAMC are described in Stachowiak et al. [1996a, 1997a] and Peng et al. [2001, 2002].

For confocal microscopy cells were plated at 95% confluency on 22 mm #1 square coverslips placed in 6-well plates (Corning Incorporated, Corning, NY). Cells were transfected by adding 4 μg of DNA and 5 μl of Lipofectamine 2000 (Invitrogen, Carlsbad, CA) to a total volume of 2.5 ml of Opti-MEM (Invitrogen) per plate. Four hours later the medium was replaced with MEM containing fetal calf serum (FCS) and antibiotics. For Western blotting, cells were plated at 95% confluency in 100-mm tissue culture plates (Corning Incorporated) and transfected with 32 μg of DNA and 10 μl of Lipofectamine 2000 in a total volume of 5 ml of Opti-MEM. Unless otherwise stated, cells were analyzed by confocal microscopy or harvested at 20 h from the onset of transfection.

Plasmid Construction

pcDNA3.1-FGFR1 vector was constructed [Peng et al., 2001] by cloning the 2,494 bp XbaI cDNA fragment containing the entire coding sequence of the three-loop form of human FGFR1 [Hou et al., 1991] into the XbaI site 3′ to the cytomegalovirus (CMV) immediate early promoter of the pcDNA 3.1 plasmid (Invitrogen). pcDNA3.1/Myc/HisB-FGFR1 was constructed by PmeI and HindIII fragment of pcDNA3.1 FGFR1 into pcDNA3.1myc/HisB cut with EcoRV and HindIII. The difference between FGFR1 and FGFR1M/H is the deletion of the terminal 30 a.a. that had no effect on subcellular localization or biological activity [Peng et al., 2001, 2002]. Construction of FGFR1 mutants is shown schematically on Figure 1. All TM mutants were constructed by PCR using the common forward primer PIII(5′-GCC AAG ACA GTG AAG TTC AAA TGC-3′) upstream from the EcoRI site (bp 52). All of the reverse primers included desired mutation and KpnI site. pcDNAFGFR1/4-Myc/His incorporated the following reverse primer PIV (5′-GCG GCG GCG GGT ACC ACT CGC CTG CCC TCG ATA CAG CCC GGC CAG CAG CAG GAG CAC AGC CAA GGC CAG GGA GCC CGA CGC GTA CAG GAT GAT GTC CGT ATA CCT GGC CAT CAC TGC CGG CCT CTC TTC CAG-3′). It corresponds to FGFR4 TM a.a. 370–400. pcDNA3.1FGFR1(Δ1-3)-Myc/His was made using the following reverse primer PIV (5′-ATC ATC ATC TAT GCGACA GGG GCC TTC GAC ATC TCC TGC ATG GCC GGG TCG GTC ATC GTC TAC AAG ATG AAG AGT GGT ACC-3′) that incorporated one mutation (V391) in FGFR1(Δ1), two mutations (V391R and C381R) in FGFR1(Δ2), and three mutations (V391R,

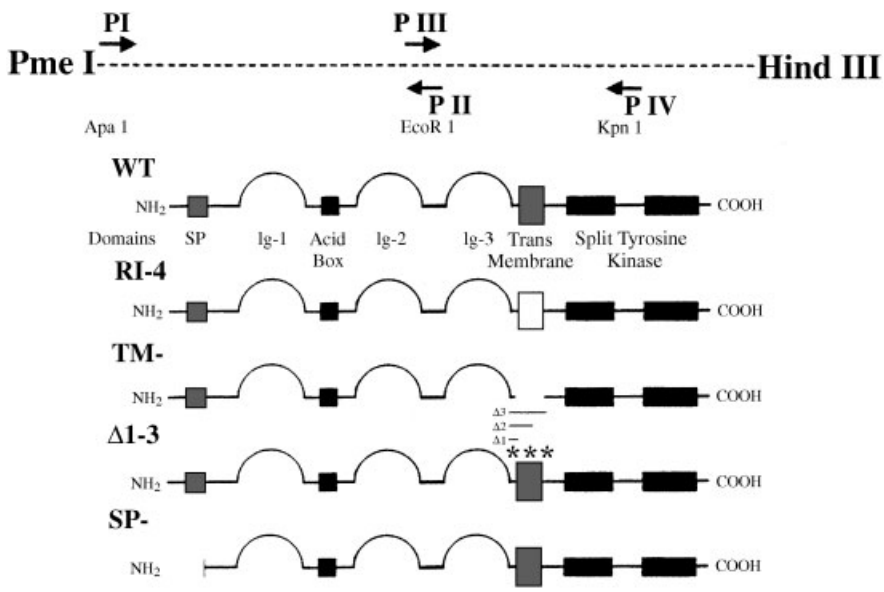

Fig. 1. Construction of mutations targeting the transmembrane domain (TM) and signal peptide (SP) domains of FGFR1. Protein structure (**bottom**) and corresponding DNA (**top**) are shown. All mutants were constructed by PCR as described in Materials and Methods. Arrows show location of primers (PI-IV). Chimeric FGFR1/4-EGFP was constructed by replacing the FGFR1 TM with the TM of FGFR4. FGFR1(TM−)-EGFP has a deleted TM (370–400 a.a.). In FGFR1(Δ1-3) TM, one (V391), two (V391R and C381R), or three (V391R, C381R, and L386) hydrophobic amino acids (a.a.) were replaced with polar a.a. to decrease TM hydrophobicity (see Materials and Methods). In FGFR1(SP−)-EGFP a.a. 3–16 of the SP are deleted to render its protein synthesis on free ribosomes.

C381R, and L386) in FGFR1(Δ3). PCR products generated with Deep Vent polymerase (New England Biolabs, Beverly, MA) were digested with KpnI and EcoRI and cloned into pcDNA3.1FGFR1-Myc/HisB cut with KpnI and EcoRI. pcDNA3.1FGFR1(SP−) was constructed by deleting the SP (a.a. 3–16) using the forward primer PI (5′-GCG GCG GGG CCC ATG TGG deleting a.a. 3–16 TGC ACC GCT AGG CCG TCC CCG AC-3′) which contained an ApaI restriction site and the reverse primer PII (5′-AGG GCA CCA CAG AGT CCA TTA TGA T-3′) downstream from the EcoRI cut site (bp 52). PCR generated product was digested with EcoRI and ApaI and cloned into pcDNA3.1FGFR1-Myc/His cut with EcoRI and ApaI. FGR1 mutants were subcloned into pEGFP-N2 from pcDNA3.1FGFR1-Myc/HisB with Hind III and PmeI restriction enzymes. All clones were verified by DNA sequencing and Western blotting to confirm correct size protein. All FGFR1 mutants are schematically shown on Figure 1.

Isolation of Membrane and Cytosolic Fractions and Western Immunoblotting

Cells were harvested in 1 ml of 20 mM Tris-HCl pH 8.0 buffer containing 2 μM PMSF, 10 μg/ml benzamadine, 1 mM EDTA, and 1 mM EGTA, collected in a 2 ml glass Dounce homogenizer and left on ice for 15 min to swell. Next the cells were sheared 30–40 times with a tight fitting teflon pestle. The homogenates were combined with 1 ml of 1 M sucrose in 20 mM Tris-HCl pH 8.0 buffer, mixed and spun at 1,600*g* for 10 min to remove nuclei. The cytoplasmic fraction was collected above the sucrose cushion cleared by centrifugation at 2,500*g* for 5 min to pellet unbroken cells and contaminating nuclei. The obtained cytoplasm was spun at 150,000*g* for 30 min in an Optima TLX ultracentrifuge (Beckman, Palo Alto, CA) in a TLS-55 swinging bucket rotor. The supernatant was concentrated in an Ultrafree-4 Centrifugal filter and Tube with a BIOMAX-30K NMWL Membrane (Millipore, Bedford, MA) to a volume of 40 μl. To the 40 μl concentrated cytosol (S150) 20 μl of 3× sample buffer was added, samples were denatured at 95°C for 10 min. The generated pellet (P150, membrane microsomal fraction) was washed by resuspending in harvest solution and spun at 150,000*g* for 30 min. The pellet was resuspended in 60 μl of 1× sample buffer and samples were boiled at 95°C for 10 min. In order to asses whether FGFR1 in the P150 fraction was membrane associated, cells were harvested in 20 mM Tris-HCl pH 8.0 buffer (supplemented with 0.1% Triton X-100), vortexed briefly, and spun at 1,600*g* though 1 M sucrose to pellet nuclei. The S150 and P150 fractions were isolated as described above. Total cell lysates were prepared by lysing the cells directly in 1× Laemli sample buffer. The lysates were denatured 95°C for 10 min and spun at 100,000*g* for 10 min to pellet DNA.

Denatured proteins were resolved on 7.5% SDS–PAGE gel with prestained protein standards (BioRad, Palo Alto, CA). The proteins were then transferred overnight onto a nitrocellulose membrane in 25 mM Tris, 192 mM glycine, and 20% methanol at 4°C. The membrane was blocked in tris buffered saline (TBS) plus 5% non-fat dry milk (Carnation, Solon, OH). Next the membranes were incubated overnight at 4°C with primary antibody anti-enhanced green fluorescent protein (anti-EGFP) JL-8 monoclonal Ab (Clontech, Palo Alto, CA) or FGFR1 specific McAb6 [Hanneken et al., 1995] diluted 1:1,000 with blocking solution. After washing with TBS containing 0.1% Tween 20, blots were incubated for 1 h at room temperature with blocking solution containing goat anti-mouse IgG (Fc) horseradish peroxidase (Pierce, Rockford, IL) diluted 1:20,000 (anti-EGFP) or 1:6,000 (McAb6). The membranes were washed in TBS and 0.1% Tween 20. Chemiluminescent detection was preformed using manufacturer's protocol (Supersignal West Pico Kit, Pierce).

Confocal Microscopy and Image Analysis

Coverslips with live cells were mounted with MEM containing 5% FCS and 1% Penn/Strep at RT and sealed with VALAP (1:1:1; low melting point paraffin, vaseline, and lanolin). Confocal images of live transfected cells were acquired using a Biorad MRC 1024 confocal microscope with a 15 mW krypton/argon laser, operating on a Nikon Optiphot upright microscope and an oil immersion 60× 1.4NA objective. Optical sections were acquired at 0.5 μm steps and the XY pixel size was set at ≥0.20 μm using BioRad's Lasersharp V3.0 software and later processed using Todd Brelje's Confocal Assistant v4.02. Fluorescence intensity measurements were performed using NIH's ImageJ V1.23q software.

The intensity of FGFR1–EGFP fluorescence associated with plasma and nuclear membranes was estimated by plotting fluorescence intensity profiles across the membrane and reading the peaks (Fig. 7A). However, instead of transecting lines, we used rectangular boxes of at least 12 pixels width, which produced more consistent and reliable readings. Also, non-cellular background was estimated and subtracted to the image before analysis. This was repeated in several optical sections and care was taken to avoid areas in which FGFR1–EGFP fluorescent cytoplasmic vesicles are adjacent to the membranes.

The cytosolic and intranuclear compartments were similarly sampled each within several random areas as described in Baumann et al. [2001], with the non-cellular background pixel intensities subtracted. Mean fluorescent intensities for the sampled compartments (MFIc) and of the entire confocal section (MFIe) were determined. The relative fluorescence intensities (RFI) of individual compartments (RFIc) were then calculated using the formula: RFIc = MFIc/MFIe.

RESULTS

Biotynylation of surface proteins in glioma or TE671 cells did not lead to the appearance of biotin-tagged FGFR1 in the nucleus indicating that nuclear FGFR1 is not derived from the cell surface [Peng et al., 2001]. On the other hand, the presence of glycosylated nuclear FGFR1 indicates that nuclear FGFR1 is processed at least partially through the golgi-ER [Stachowiak et al., 1997b]. To examine whether FGFR1 may be released from the ER membranes into the cytosol prior to its nuclear uptake we followed the localization of FGFR1–EGFP in live TE671 cells at different time points after transfection. At 12 h, intense FGFR1–EGFP fluorescence was noted in the cytoplasm. In several cells examined, these highly fluorescent bodies were associated with golgi-ER-like vesicles as shown by superimposition of confocal and phase-contrast images (Fig. 2A, arrows), plasma and nuclear membranes, and thin filopodia [Fig. 2 (*)]. However, no FGFR1–EGFP fluorescence was observed in non-membrane regions of the cytoplasm, outside vesicles, and the nuclear interior (Fig. 2A, arrowhead). At 26 h, fluorescence associated with the golgi-ER decreased, cytosolic fluorescence increased, and FGFR1–EGFP accumulated in the nucleus (Fig. 2A), except in nucleoli (Fig. 2A–C—confocal section through nucleoli). At 40 h, fluorescence became more evenly distributed and throughout the cell (Fig. 2A), and association of FGFR1–EGFP with the nuclear and plasma membrane was no longer distinguishable. This initial experiment showed that accumulation of FGFR1–EGFP in the cytoplasmic membranes precedes the accumulation in the cytosolic-like compartment and in the nuclear interior.

Nuclear accumulation of FGFR1–EGFP in TE671 cells could be a result of nuclear membrane fragmentation during karyokinessis, due to the fact that these cells divide rapidly (doubling time of approximately 12 h). Therefore, FGFR1–EGFP trafficking in non-proliferating post-mitotic BAMC (Fig. 2B) and in slowly proliferating SF763 glioma cells (Fig. 2C) was examined. Forty hours after BAMC transfection the presence of FGFR1–EGFP fluorescence within the nucleus, cytosol, golgi-ER (arrows), nuclear and plasma membranes, and filopodia was observed (*) (Fig. 2B). FGFR1–EGFP had a relatively homogenous distribution in SF763 cells similar to TE671 cells 40 h after transfection. The association of FGFR1–EGFP with plasma or nuclear membranes no longer could be distinguished at this time. Thus, nuclear accumulation of FGFR1–EGFP occurs in different cells and is independent of their proliferative activity. All subsequent experiments were performed in SF763 cells analyzed 20 h after transfection. The accumulation of FGFR1–EGFP in golgi-ER, cytosol, and the nuclear interior of BAMC or SF763 followed a similar sequence and time course to TE671 (not shown). This sequence was consistent with the current knowledge that proteins containing SPs are destined to constitutively associate with membranes or undergo regulated secretion. Furthermore, it suggested that FGFR1–EGFP is released from the cytoplasmic membranes into the cytosol before its accumulation in the nucleus. Hence, we turned our attention to the FGFR1 TM for receptor mobilization.

Homology and Structure of TM Within the Family of FGFR

The crystal structure of only a portion of the FGFR1 molecule (142–365 a.a.) containing immunoglobin-like has been characterized

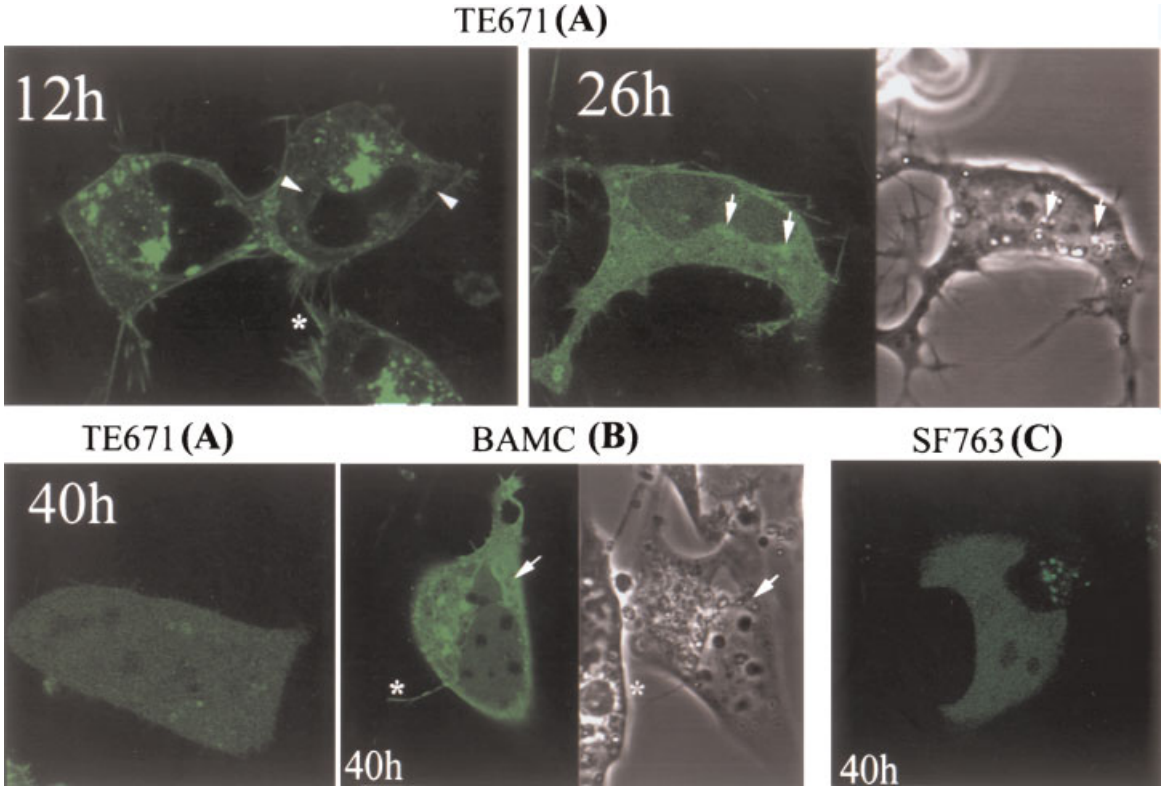

Fig. 2. FGFR1–EGFP is present in the cell nucleus independent of mitotic activity. **A**: TE671 medulloblastoma (doubling time approximately 12 h)—subcellular trafficking of FGFR1–EGFP at 12, 26, and 40 h post-transfection. **B**: Bovine adrenal medullary cells (BAMC) (post-mitotic cells)—40 h after FGFR1–EGFP transfection. **C**: SF763 glioma cells (doubling time approximately 2 days)—40 h after FGFR1–EGFP transfection. Confocal and phase contrast images show approximately mid-cell levels. Arrowheads indicate cytosolic regions devoid of fluorescence (TE671, 12 h); arrows indicate golgi-ER vesicles; asterisks indicate filopodia. Live cells were imaged as described in Materials and Methods. [Color figure can be viewed in the online issue, which is available at www.interscience.wiley.com].

[Plotnikov et al., 1999]. Therefore, we applied Garnier algorithms [Reyes et al., 1989; Viswanadhan et al., 1991] to predict the conformation of the TM domains in FGFR1-4. The TM domain typically forms a hydrophobic α-helical structure. These hydrophobic moieties interact with the lipid bilayer and anchor the protein in the membrane. The TM domains in FGFR1-4, identified by hydrophobicity/hydophilicity plots, contain 27, 29, 29, and 22 a.a. (Fig. 3A) [Hou et al., 1991; Keegan et al., 1991; Partanen et al., 1991]. The TM of FGFR1 and 2 display the largest degree of homology (60%), while the TM sequences of FGFR1, 2, and 3 show 30% homology. All four FGFR display only a 7% homology (Fig. 3A). The TM also differ in the number of hydrophobic a.a FGFR3(21) > FGFR2(21) > FGFR4(17) = FGFR1(17). Furthermore, FGFR1 has the shortest continuous runs of hydrophobic a.a (Fig. 3A,B). Garnier algorithms (Fig. 3C) predict a typical α-helical structure for the FGFR4 TM, FGFR2, and FGFR3 both have β-sheet regions followed by shorter α-helices, however, the TM domain of FGFR1 has a β-sheet-turn-β-sheet structure with no predicted α-helix.

Characterization of FGFR1–EGFP Fusion Proteins Expressed in SF763 Cells

The following FGFR1 receptor mutants were designed to examine the significance of the TM in the nuclear accumulation of FGFR1 (Fig. 1). In the chimeric receptor FGFR1/4 the predicted atypical β-sheet TM of FGFR1 was replaced with the α-helical TM of FGFR4. In FGFR1(Δ1)(V391R), FGFR1(Δ2)(V391R and C381R), and FGFR1(Δ3)(V391R, C381R, and L386D) 1, 2, or 3 hydrophobic a.a. were replaced with hydrophilic a.a., respectively, to decrease TM hydrophobicity. In FGFR1(TM−) the entire TM (370–400 a.a.) was deleted. Along with the TM mutants, we constructed FGFR1(SP−) with the SP, a.a. 3–16, deleted. In order to follow the subcellular distribution of

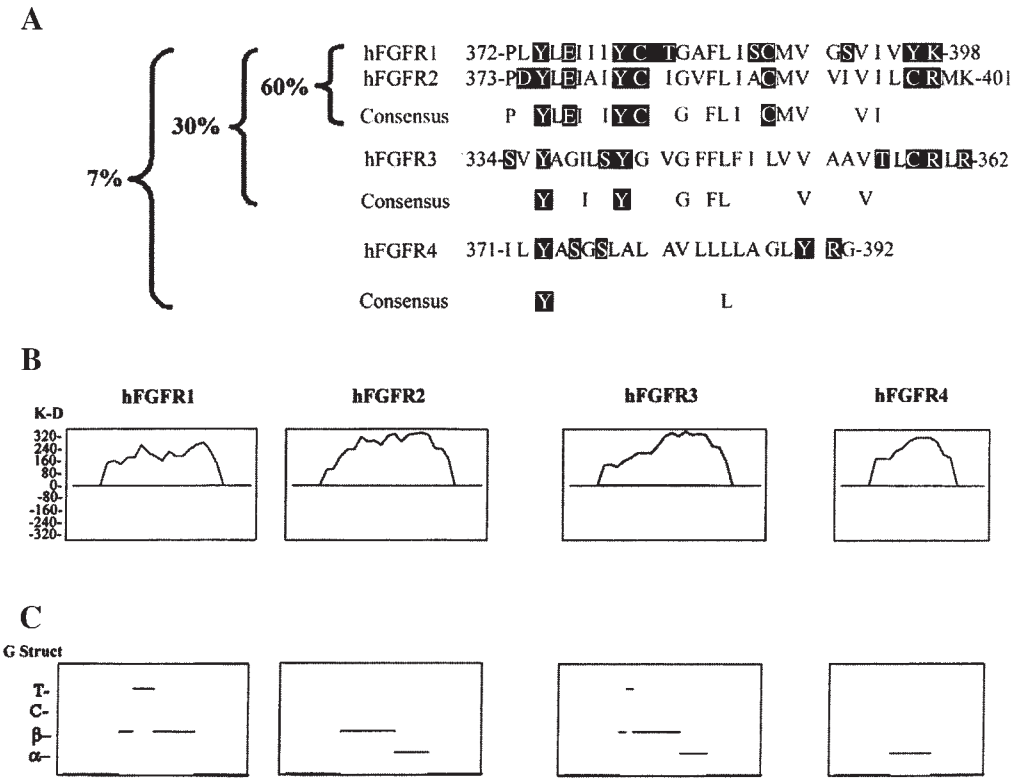

Fig. 3. Sequence analysis of TM in FGFR1-4. **A**: TM homology among FGFR1-4. Polar a.a. are indicated by inverted characters, respectively. FGFR1 has the shortest continuous runs of hydrophobic a.a. These features are reflected in the respective TM hydrophobicity plots **(B)**. **C**: Chou-Fasman and Garnier algorithms predict the TM of FGFR4 to be a typical α-helix. In contrast FGFR1 showed a β-sheet-turn-β-sheet structure with no predicted α-helix. Both FGFR2 and FGFR3 demonstrated β-sheets followed by shorter α-helices. (α = α-helics; β = β-sheet; T = turn, C = random coil).

these proteins in live cells, wild type FGFR1 and each of its mutants were cloned in frame into the EGFP vector with the 35 C-terminal FGFR1 a.a. deleted and the remaining C-terminal end connected to the N-terminal end of EGFP (see Materials and Methods). Neither the gene-transactivating function of wild type FGFR1 nor the subcellular distribution of FGFR1 and its mutants were affected by the a.a. deletion and fusion to EGFP [Peng et al., 2001, 2002]. SF763 cells were transfected with equal amounts of plasmids expressing wild type FGFR1–EGFP, FGFR1–EGFP mutants, or control EGFP or tubulin-EGFP to confirm pEGFP fusion proteins. Twenty hours after transfection SF763 cells were solubilized and total cell proteins subjected to Western analysis with anti-EGFP MAb. The EGFP protein expressed from control vector pEGFP migrated 27 kDa (Fig. 4; lanes 1, 8, and 12), while tubulin-EGFP approximately 80 kDa (Fig. 4; lanes 7, 11, and 15) consistent with the combined molecular weight of tubulin (50 kDa) and EGFP. Untagged wild type FGFR1 migrates as the most abundant 105 kDa and additional 95 and 135 kDa bands, which correspond to hypoglycosylated, non-glycosylated and hyperglycosylated forms of FGFR1, respectively [Stachowiak et al., 1997b; Peng et al., 2001, 2002]. Wild type FGFR1 in frame with EGFP migrated at 135 kDa (Fig. 4; lanes 2, 9, and 14). Similar to non-tagged FGFR1, treatment with *N*-glycanase reduced the size of FGFR1–EGFP by approximately 5–10 kDa (not shown). Thus, the 135 kDa band represents EGFP fusion with the most abundant partially glycosylated 110 kDa FGFR1. The primary band seen in FGFR1/4-EGFP (lane 3) and FGFR1(Δ1)-EGFP (lane 10), FGFR1(Δ2)-EGFP (lane 5), and FGFR1(Δ3)-EGFP (lane 6) co-migrated with the wild type at 135 kDa FGFR1–EGFP.

FGFR1(TM−)-EGFP lacks 30 a.a., but undergoes glycosylation (our unpublished observations), and has a slightly reduced size of 128 kDa (Fig. 4, lane 4). Additional hyperglycosylated isoforms for FGFR1–EGFP, FGFR1/4-EGFP,

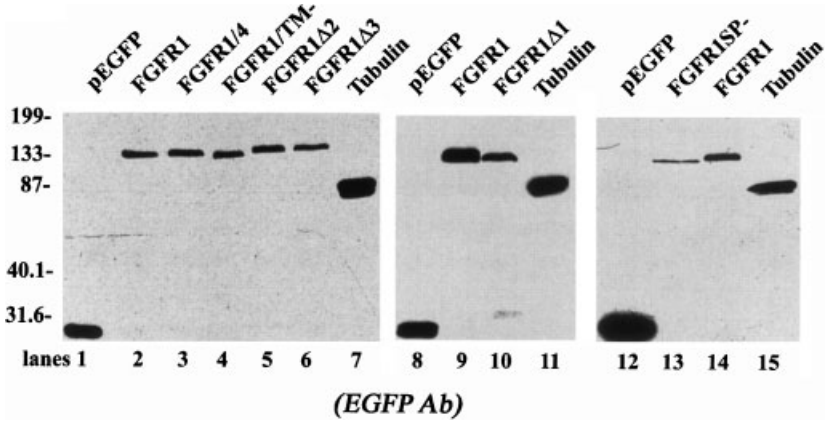

Fig. 4. Western immunoblot analysis of FGFR1–EGFP fusion proteins in total cell lysates. FGFR1–EGFP and controls were transfected into SF763 cells. At 20 h post-transfection cells were lysed in sample buffer and analyzed by Western blot with an anti-EGFP MAb. The control EGFP migrates at 27 kDa (**lanes 1**, **8**, and **12**) and tubulin-EGFP at 80 kDa (**lanes 7**, **11**, and **15**). FGFR1-EGFP (**lanes 2**, **9**, and **14**), FGFR1/4-EGFP (**lane 3**), FGFR1(Δ1)-EGFP (**lane 10**), FGFR1(Δ2)-EGFP (**lane 5**), and FGFR1(Δ3)-EGFP (**lane 6**) all migrated at 130 kDa. FGFR1(TM−)-EGFP (**lane 4**) has a slightly reduced size of 128 kDa. FGFR1(SP−) (**lane 13**) runs as a single band around 128 kDa. Additional hyperglycosylated isoforms of FGFR1–EGFP, FGFR1/4-EGFP, FGFR1(TM−)-EGFP, and FGFR1(Δ1-3)-EGFP were observed with longer exposure (not shown) or in more sensitive assay using FGFR1 McAb6 (Fig. 5).

FGFR1(TM−)-EGFP, and FGFR1(Δ1-3)-EGFP, but not FGFR1(SP−) are visible with longer exposure times and when isolated membrane and cytosolic fractions were analyzed (Figs. 5 and 6). FGFR1(SP−)-EGFP migrated as a single band of 128 kDa (Fig. 4, lane 13) consistent with the size of a non-glycosylated fusion protein. Since the SP is normally cleaved during membrane insertion, the size of FGFR1(SP−) should be the same as nascent (non-glycosylated) FGFR1. Extracts of cells expressing FGFR1 fusion proteins or tubulin-EGFP contained no additional lower molecular weight bands that would indicate an expression of EGFP alone (27 kDa) or fragments of FGFR1–EGFP or tubulin-EGFP proteins from the transfected recombinant plasmids.

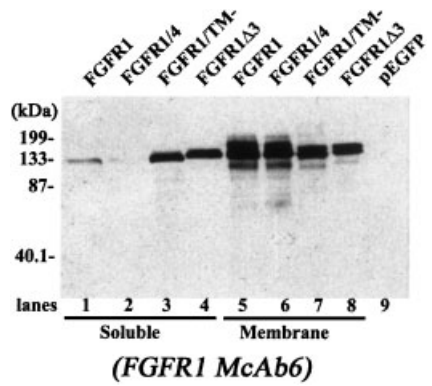

Fig. 5. Distribution of FGFR1–EGFP protein in soluble cytosolic (S150) and microsomal membrane (P150) fractions—Western analysis with anti-FGFR1 McAb6. Levels of endogenous FGFR1 were not detectable in total cellular protein of pEGFP transfected cells (**lane 9**). McAb6 detected membrane-associated FGFR1–EGFP, FGFR1/4-EGFP, FGFR1(TM−)-EGFP, and FGFR1(Δ3)-EGFP (**lanes 5**, **6**, **7**, and **8**). In the cytosolic fraction, McAb6 detected relatively small amounts of soluble FGFR1–EGFP (**lane 1**) and only trace of FGFR1/R4-EGFP (**lane 2**). The amounts of FGFR1(TM−)-EGFP and FGFR1Δ3-EGFP in the cytosolic and microsomal fractions were similar (**lanes 3** and 7, **4** and 8). Additional hyperglycosylated 150 and 165 kDa isoforms were detected only in P150 fraction.

Mutations of the TM Affect FGFR1 Subcellular Localization

The purpose of FGFR1–EGFP mutations was to alter the receptor association with cellular membranes. Transfected w.t. FGFR1–EGFP and its mutants were analyzed for their association with microsomal membrane (P150) and soluble cytosolic (S150) fractions in SF763 cells (Fig. 5) by immunoblotting with anti-FGFR1 McAb6. Total cellular protein from cells transfected with pEGFP were analyzed to ascertain the specificity of McAb6 and in the present study, similar as in Stachowiak et al., 1997a the levels of endogenous FGFR1 were not detectable in pEGFP-transfected SF 763 cells (Fig. 5, lane 9).

FGFR1(TM−)-EGFP and FGFR1(Δ3) accumulated to a similar extent in the P150 membrane fraction (Fig. 5; lanes 7, 8), and in the soluble S150 fraction (Fig. 5; lanes 3, 4). Single bands were detected for the FGFR1Δ3-EGFP

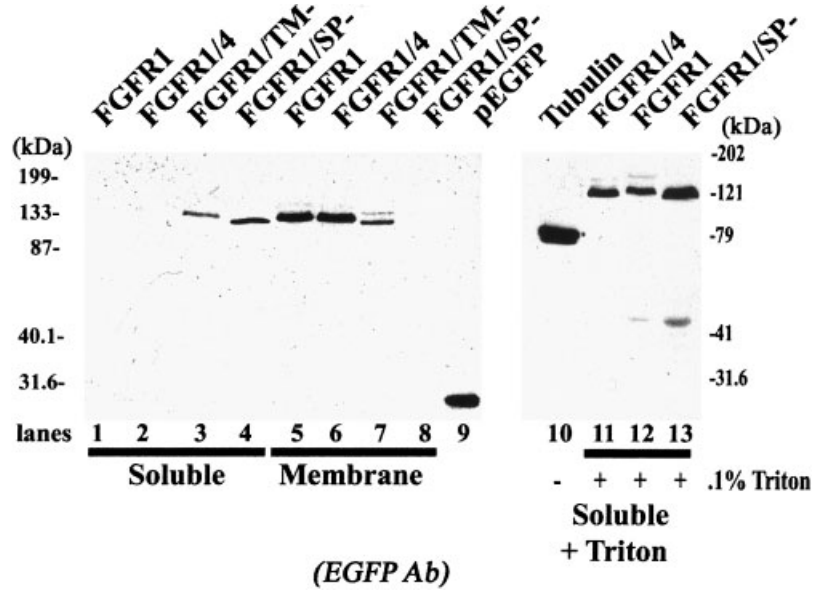

Fig. 6. Release of FGFR1–EGFP and FGFR1/4-EGFP into cytosol by 0.1 % Triton X-100. SF763 cells were transfected with FGFR1–EGFP or its mutants. Microsomal membrane (P150) and soluble cytosolic (S150) fractions were isolated 20 h post-transfection and were immunoblotted with anti-EGFP Ab. Total cellular protein from cells transfected with pEGFP were also analyzed to ascertain the specificity of anti-EGFP MAb (**lane 9**). EGFP MAb immunoblotting assay was less sensitive than the immunoblotting with FGFR1 McAb6 (Fig. 5) and FGFR1 in S150 fraction was detected only after a long exposure (not shown). To verify the (P150) fraction association of FGFR1 and FGFR1/4 could be shifted to the (S150) fraction cells were lysed in a buffer containing 0.1% Triton X-100 (**lanes 11**, **12**, **13**). As a marker for the cytosolic fraction transfected resident soluble protein FGFR1(SP−)-EGFP was analyzed. No receptor-EGFP protein was detected in P150 of cells lysed with 0.1% Triton X-100.

(135 kDa) and FGFR1(TM−)-EGFP (128 kDa) mutants in the S150 fraction, while in the P150 fraction the mutants presented two additional bands, 150 and 165 kDa, respectively. In contrast, the amount of FGFR1–EGFP associated with the P150 fraction (Fig. 5, lane 5) was several-fold greater than the amount detected in the S150 fraction (Fig. 5, lane 1). FGFR1/R4-EGFP was present nearly exclusively in P150 fraction, with no or only trace amounts of FGFR1/R4-EGFP in S150 fraction (Fig. 5; lanes 2, 6). Only the 135 kDa hypoglycosylated isoform of FGFR1–EGFP, FGFR1(TM−)-EGFP, and FGFR1Δ3-EGFP was detected in the S150 fraction. Similar results were obtained using anti-EGFP MAb (Fig. 6).

To verify that the (P150) fraction contained membrane associated FGFR1–EGFP and FGFR1/4-EGFP, cultured cells were collected in a harvest buffer containing 0.1% Triton X-100. Fractions corresponding to P150 and S150 were isolated along with fractions obtained without 0.1% Triton X-100, analyzed by Western immunoblotting with anti-EGFP MAb (Fig. 6). As a marker for the cytosolic fraction, the resident soluble protein FGFR1/SP− was also analyzed. FGFR1(SP−)-EGFP was present in large amounts in the S150 fraction (lane 4) but was not detected in P150 fraction (lane 8). Addition of the non-ionic detergent shifted FGFR1/4-EGFP and FGFR1–EGFP to the S150 fraction (Fig. 6; lanes 11, 12). No FGFR1–EGFP or FGFR1/R4-EGFP was detected in P150 of 0.1% Triton X-100 treated cells (not shown).

Effect of FGFR1 Mutations on Membrane, Cytoplasmic, and Nuclear Association of FGFR1–EGFP in Live Cells

Like the endogenous FGFR1 [Stachowiak et al., 1996a,b; Peng et al., 2001, 2002], transfected FGFR1–EGFP accumulates in five distinct compartments: (1) plasma membrane, (2) nuclear membrane, (3) perinuclear golgi-ER vesicles distinguishable by phase contrast microscopy, (4) nuclear interior, (5) non-vesicular diffuse FGFR1–EGFP in peripheral cytoplasm. The mean intensities of the fluorescence associated with the plasma and nuclear membranes were estimated as described in Materials and Methods. The perinuclear golgi-ER fluorescence was analyzed by outlining the

contours of vesicles and measuring the mean fluorescence of the enclosed areas. This was not done in cells expressing FGFR1(SP−)-EGFP as this protein did not associate with golgi-ER structures. The cytosolic compartment was sampled randomly by outlining several non-membranous peripheral cytoplasmic areas outside the golgi-ER and determining their mean fluorescence intensities. Similarly, the mean fluorescence of the entire nuclear interior with the exception of nucleolus, was calculated. This analysis was performed on randomly selected cells in at least three independent transfection experiments. To account for the different overall levels of FGFR1–EGFP expression in different cells (and with different FGFR1 mutants) and slight photobleaching observed during repetitive confocal scans, we calculated RFI of each compartment by dividing their mean fluorescence intensity by the mean fluorescence intensity of the whole cell within the analyzed confocal section after background (non-cellular) pixel intensity was subtracted.

In SF763 cells, no distinct peaks were observed on the intensity plots encompassing the region from the extracellular space to the peripheral cytoplasm, indicating that FGFR1–EGFP did not accumulate in the plasma membrane (Fig. 7A). This is in contrast to TE671 cells, where an association was observed (Fig. 2A). Nuclear membrane-associated FGFR1–EGFP was observed as a distinct peak (Fig. 7A).

This analysis showed the presence of FGFR1–EGFP in the nuclear membrane (RFI = 2.8), golgi/ER (RFI = 6.2), nuclear interior (RFI = 0.38), and cytosol (RFI = 0.4). FGFR1–EGFP RFI in plasma membrane region was at background levels (RFI < 0.1).

The whole cell mean fluorescence intensity was similar in cells transfected with wild type FGFR1–EGFP, FGFR1/R4-EGFP, FGFR1(Δ1)-EGFP, FGFR1(Δ2)-EGFP. Mean fluorescence intensity was slightly higher in cells expressing FGFR1Δ3-EGFP, FGFR1 (SP−)-EGFP, or FGFR1(TM−)-EGFP (Fig. 7B); these results are consistent with the results of Western blot analysis in total cell lysates (Fig. 4). The obtained RFI of individual compartments are shown on Figure 7B. The chimeric protein FGFR1/4-EGFP was associated with the golgi-ER and nuclear membranes (Fig. 7A,B), where the RFI values of FGFR1–EGFP and FGFR1/R4-EGFP were essentially the same. The FGFR1/R4-EGFP fluorescence accumulated in the plasma membrane, in contrast to w.t. FGFR1–EGFP and all remaining FGFR1 mutants. The FGFR1/R4 mutation reduced RFI in the cytosol and in the nuclear interior to near background levels (Fig. 7A,B) that were significantly lower (twofold to fourfold) than FGFR1–EGFP (Fig. 7A,B). Thus, the replacement of the FGFR1 TM with that of FGFR4 produces a receptor associated with the cell surface and intracellular membranes, but which is depleted from the cytosol and the nuclear interior.

To further establish the relationship between receptor mobility and cytosolic and nuclear accumulation, FGFR1 mutants with increasing TM polarity were used. The (V391R) mutation in FGFR1(Δ1)-EGFP occurs naturally in FGFR3 in association with achondroplasia resulting in constitutively active FGFR3, independent of ligand binding [Shiang et al., 1994]. Subcellular localization of FGFR1(Δ1)-EGFP was similar to that of wild type FGFR1–EGFP with strong FGFR1(Δ1)-EGFP fluorescence associated with the golgi-ER, nuclear membrane, and its apparent absence from the plasma membrane (Fig. 7A,B). Fluorescence was less intense in the cytosol and nuclear interior. The comparative RFI analysis of SF763 cells expressing FGFR1(Δ2)-EGFP with point mutations (V391R and C381R) showed an increased RFI in the cytosolic-like compartment outside the golgi-ER, plasma, and nuclear membranes (Fig. 7A,B). A similar increase in the nuclear RFI in comparison with FGFR1(Δ1)-EGFP and FGFR1–EGFP was found (Fig. 7A,B). The consequences of increased TM polarity was most striking in FGFR1(Δ3)-EGFP bearing three mutations (V391R, C381R, and L386D). The golgi-ER RFI of FGFR1(Δ3)-EGFP showed further decrease with concomitant increases in cytosolic and intranuclear RFIs (Fig. 7A,B). The FGFR1(Δ3)-EGFP RFI in the nuclear membrane was lower than in the cytoplasm or nuclear interior. The nuclear membrane RFI of FGFR1(Δ3)-EGFP and FGFR1(SP−)-EGFP were not significantly different with no association in the plasma membrane (Fig. 7A). Together, these results indicate that increased TM polarity decreases association of FGFR1 with nuclear and intra-cytoplasmic membranes while increasing cytosolic and nuclear contents. In contrast, increasing the number of polar TM a.a. gradually decreased the nuclear membrane

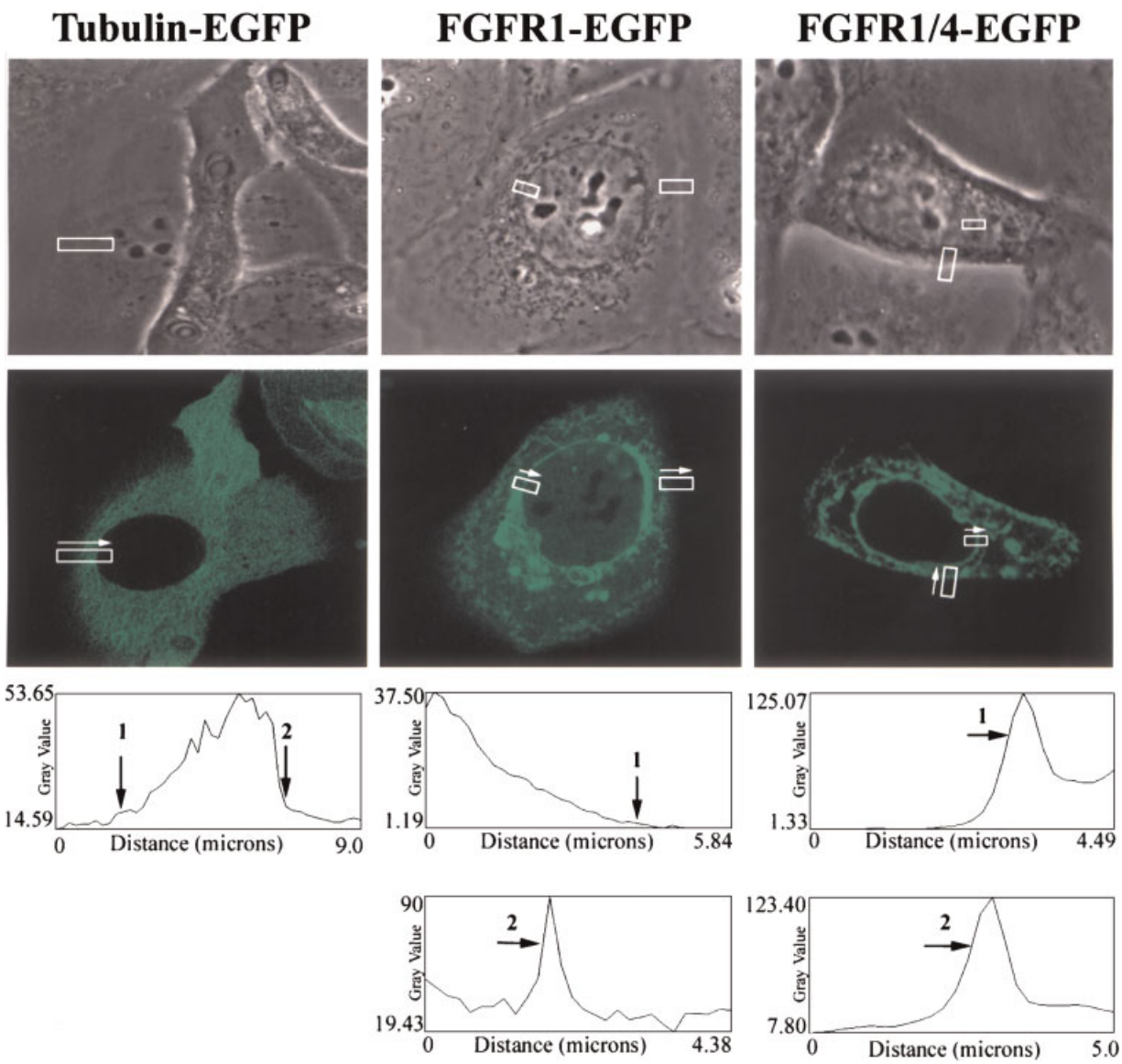

Fig. 7. Mutations in the TM affect subcellular localization of FGFR1–EGFP. **A**: Representative cells transfected with EGFP fused to w.t. or mutant FGFR1 or to tubulin. The intensity of FGFR1–EGFP fluorescence associated with the plasma (1) and nuclear (2) membrane was estimated using NIH's ImageJ V1.23q software as an average from 15–22 single pixel lines transecting perpendicularly the membrane in areas marked by white rectangles. Membrane localization is confirmed on corresponding phase contrast images. Cells transfected with tubulin-EGFP showed fluorescent microtubules but, no EGFP fluorescence was detected in the nucleus. **B**: Quantitative analysis of receptor distribution. Transfected FGFR1–EGFP was analyzed in five compartments: (1) plasma membrane, (2) nuclear membrane, (3) perinuclear golgi-ER vesicles distinguishable also by phase contrast microscopy, (4) nuclear interior, (5) non-vesicular diffuse FGFR1–EGFP in peripheral cytoplasm representing the cytosolic compartment as described in Materials and Methods. To account for the different overall levels of FGFR1–EGFP expression in different cells, we calculated RFI of each compartment by dividing their mean fluorescence intensity by the mean fluorescence intensity of the whole cell within the analyzed confocal section after background (non-cellular) pixel intensity was subtracted. RFI, multivariate analysis: overall differences between FGFR1 constructs, differences between subcellular compartments and the interaction between these two variables were all significant at $P < 0.001$. Post-hoc LSD, *; ** different from WT ($P < 0.05$; $P < 0.001$); +; ++ different from TM ($P < 0.05$; 0.001). **C**: Partition of w.t. and mutant FGFR1–EGFP between cytosolic and nuclear membrane compartments and between the cytosolic and golgi-ER compartments. Bars represent mean ± SEM ratios calculated for the individual cells used in (B) (total 45 cells used). ANOVA: overall effects of FGFR1 mutations on cytosol/nuclear membrane and cytosol/golgi ER $P < 0.001$. **D**: Correlation between FGFR1–EGFP distribution in the intranuclear and cytosolic compartments. Cells transfected with w.t. FGFR1, FGFR1/R4, or individual FGFR1Δ1,2, 3 mutants fused with EGFP. Nuclear and cytosolic RFIs were estimated for each cell and their values were subjected to linear regression analysis; $r = 0.89 \pm 0.19$. [Color figure can be viewed in the online issue, which is available at www.interscience.wiley.com].

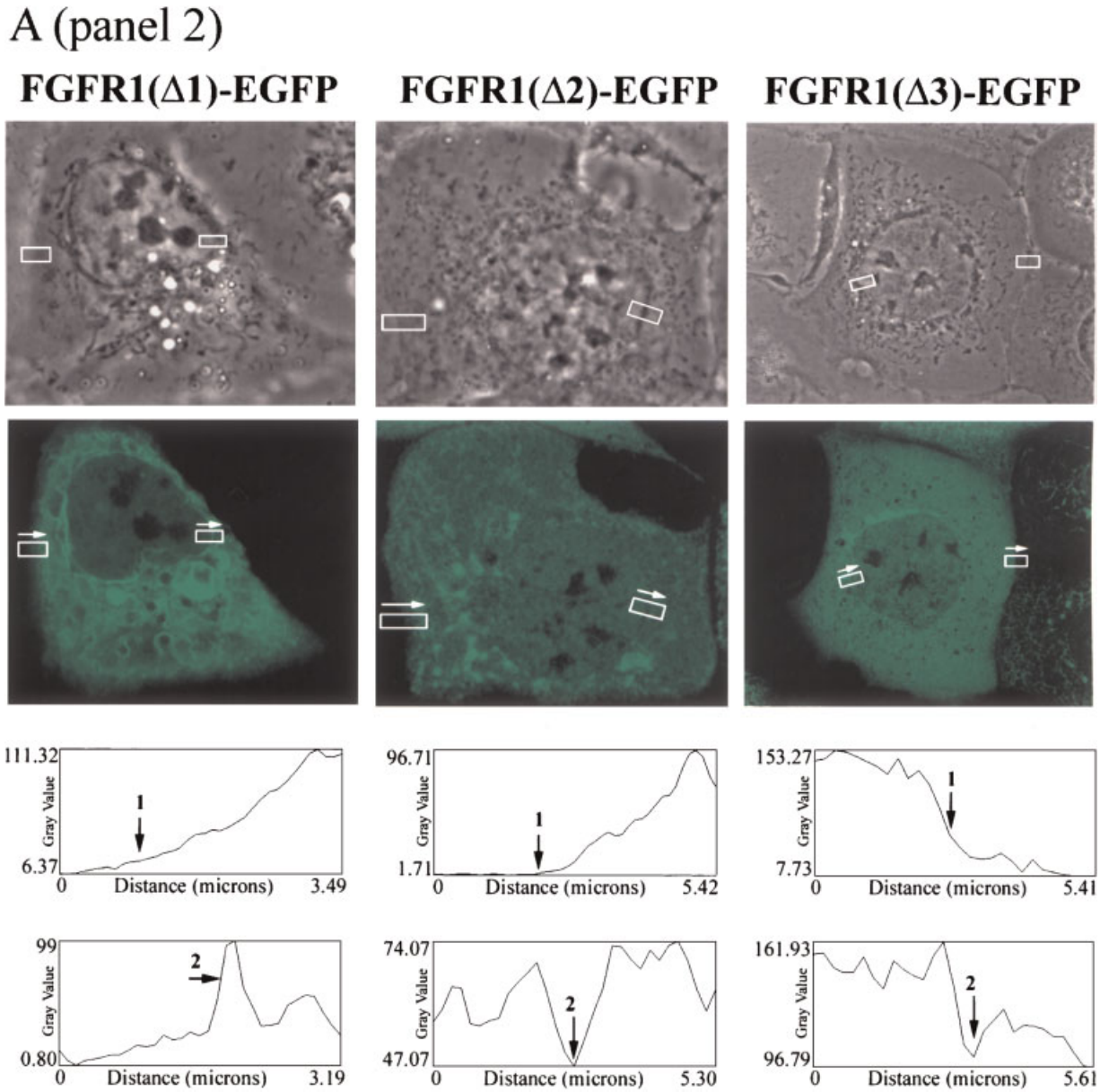

Fig. 7. (*Continued*)

and golgi-ER RFIs, while increasing the cytosolic and intranuclear RFIs.

Deletion of the TM Does Not Prevent Nuclear FGFR1 Accumulation

So far, the results suggest that the FGFR1 TM enables the receptor to enter the nucleus and that mutations that reduce TM hydrophobicity facilitate nuclear entry. To determine whether the TM functions as a NLS, directing the receptor to the nucleus, we analyzed the localization of FGFR1(TM−)-EGFP. Transfected FGFR1(TM−)-EGFP was detected in the ER, vesicles, cytosol, and the nuclear interior (Fig. 7A). With the cytosolic and nuclear RFI values similar to those of FGFR1(Δ3)-EGFP and increased relative to FGFR1−EGFP, we concluded that the FGFR1 TM is not required for nuclear accumulation of the receptor (Fig. 7B). There were no distinct peaks corresponding to the plasma and nuclear membrane on the FGFR1(TM−)-EGFP fluorescence histograms and the corresponding RFI values were similar to FGFR1(Δ3)-EGFP and FGFR1(SP−)-EGFP (Fig. 7A,B).

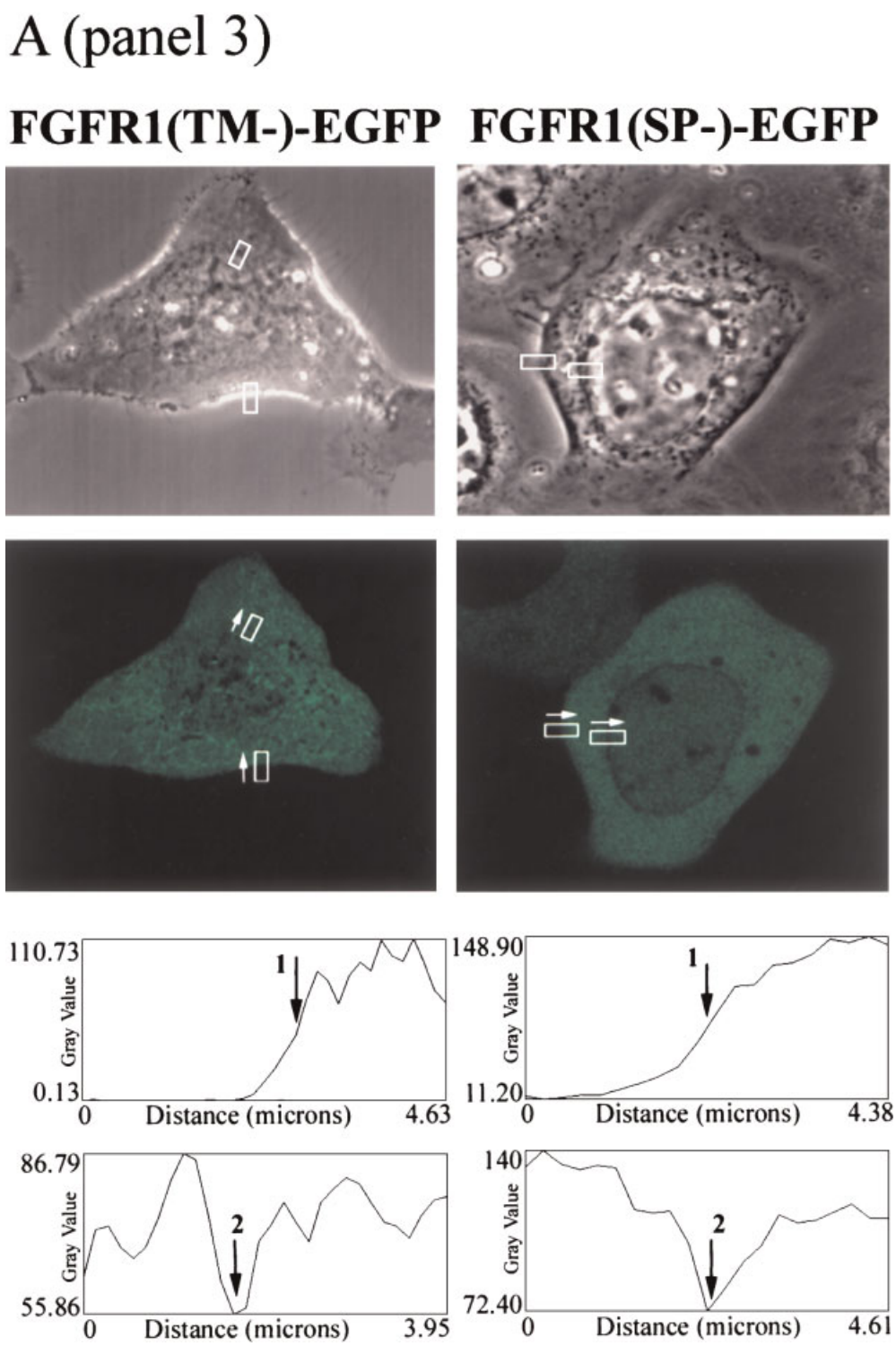

Fig. 7. (*Continued*)

Resident Soluble Cytosolic Receptor FGFR1(SP−)-EGFP Accumulates in the Cell Nucleus

To test whether a resident soluble cytosolic receptor can enter the nucleus we transfected SF763 cells with FGFR1(SP−)-EGFP. In the absence of a SP FGFR1(SP−)-EGFP should be translated by free ribosomes and thus become a soluble protein without initial insertion into the ER membrane. FGFR1(SP−)-EGFP showed a

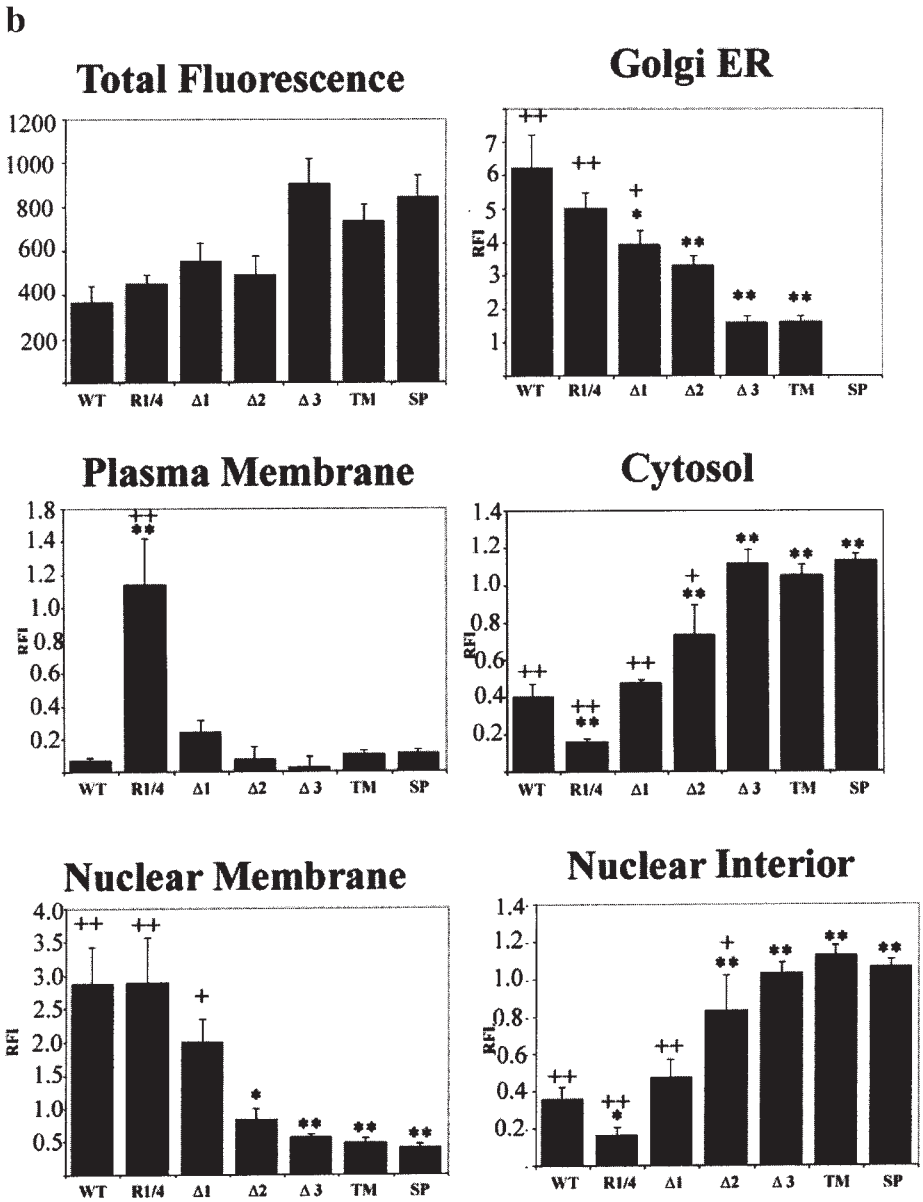

Fig. 7. (*Continued*)

homogenous distribution outside the nucleus supporting the assertion that the homogenous cytoplasmic fluorescence of FGFR1–EGFP (and all of its mutants) outside golgi-ER vesicles represents a soluble receptor. FGFR1(SP−)-EGFP was also present inside the nucleus demonstrating that the receptor can be translocated from the cytosol to the nuclear interior (Fig. 7A).

The RFI of FGFR1(SP−)-EGFP in the nuclear membrane was lower than in the cytoplasm or nuclear interior. It was also significantly reduced compared to FGFR1–EGFP, FGFR1/R4-EGFP, FGFR1(Δ1)-EGFP, and FGFR1(Δ2)-EGFP mutants and slightly diminished relative to FGFR1(Δ3)-EGFP (Fig. 7A,B). There was no detectable association of FGFR1(SP−)-EGFP with golgi-ER structures, in contrast to FGFR1(TM−)-EGFP.

Changes in FGFR1 partition between the cytosol and the nuclear membrane and between the cytosol and the golgi-ER are illustrated in Figure 7C. The nuclear membrane estimates were used since they represent a clearly defined membrane compartment. These results show shifting of FGFR1 from the membrane to the cytosolic compartment with increasing TM polarity and the opposite change when the TM

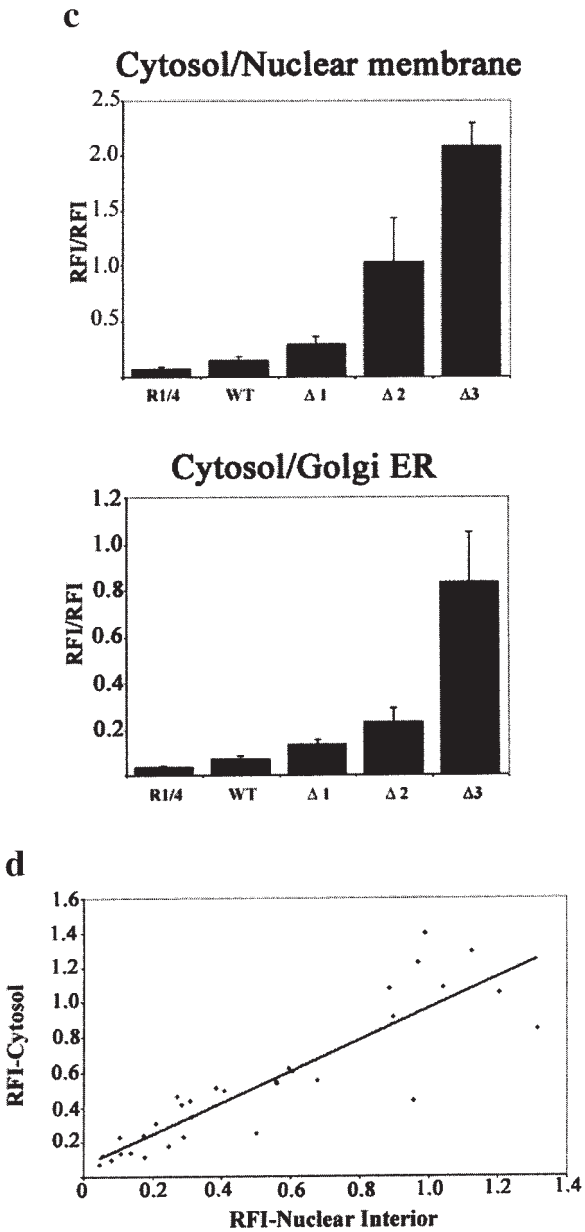

Fig. 7. (*Continued*)

of FGFR1 was replaced with FGFR4 TM. These results are consistent with biochemical analysis of FGFR1 partition between cytosolic and microsomal compartments (Fig. 5). The RFI of the nuclear and cytosolic compartments showed a significant correlation ($r = 0.89 + 0.19$) (Fig. 7D) indicating that the cytosolic and nuclear receptor pools are in equilibrium.

Proteasome Activity Influences Cytosolic Accumulation of FGFR1

Recent findings have led to the emergence of new models for the processing of transmembrane and soluble luminal proteins from the ER. Newly synthesized proteins associate with the TM Sec 61 complex, which then facilitates their retranslocation back to the cytosol through protein-conducting channels. This pathway then terminates in cytosolic proteasomes [Matlack et al., 1998]. The inhibition of a proteasome with lactacystin, a site-directed selective inhibitor of proteasomal β-type subunit [Fenteany et al., 1995], results in accumulation of transmembrane proteins that were retranslocated into the cytosol [Wiertz et al., 1996; Yang et al., 1998]. To determine whether FGFR1 may be released from the membrane via the proteasome-coupled pathway, we incubated SF763 cells with 3 μM lactacystin 20 h after transfection. Cells were harvested 4 h later and P150 and C150 fractions were isolated and immunoblotted with anti-FGFR1 McAb6. In lactacystin-treated cells an accumulation of FGFR1–EGFP in the cytosol was observed. In contrast lactacystin had no effect on the content of the resident cytosolic protein FGFR1(SP−)-EGFP (Fig. 8).

DISCUSSION

While the mechanism of the nuclear transport of cytosolic proteins are in general well characterized less is known about how TM proteins may be retrieved into the cytosol. The C-terminal fragment of the EGF receptor enters the nucleus [Lin et al., 2001] from the plasma membrane via a proteolytic process that cleaves the cytoplasmic fragment of the receptor from the rest of the membrane associated molecule [Ni et al., 2001]. However, in the case of nuclear FGFR1, the receptor is full length and FGFR1 molecules immunoprecipitated with C-terminal FGFR1 Ab can be detected on Western blots with antibody against the N-terminal Ig-loop portion of FGFR1 [Stachowiak et al., 1996a,b]. This region of the TM receptor is inside the ER lumen or on the outer surface of the plasma membrane. Glycosylation of cytosolic and nuclear FGFR1 and association of FGFR1–EGFP with golgi-ER vesicles while FGFR1(SP−) was neither golgi-ER-associated nor glycosylated, indicating that the SP-containing receptor is processed via the ER.

The present study also points to the release of the membrane receptor as an essential step in directing FGFR1 into the nucleus and sheds a new light on why FGFR1 is released from the

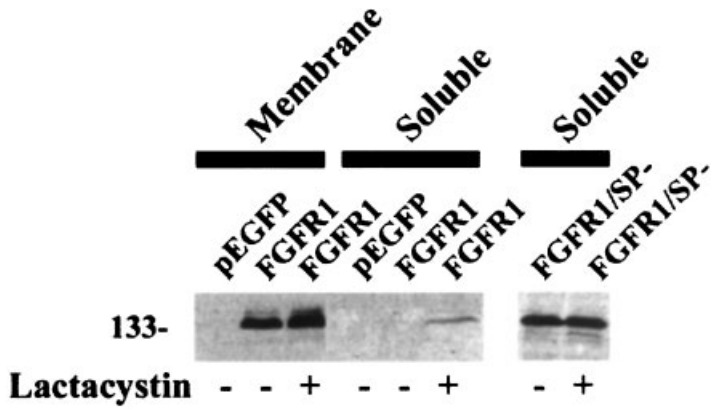

Fig. 8. Effect of lactacystin on FGFR1 content in soluble cytosolic (S150) and microsomal membrane (P150) fraction. SF763 were transfected with indicated receptor-EGFP constructs and 20 h later treated with 3 μM lactacystin for additional 4 h. P150 and S150 fractions were isolated as on Figure 5 and immunoblotted with anti-FGFR1 McAb6.

membrane. The association of FGFR1 TM with the ER membrane appears to be relatively unstable and the nucleus-destined receptor is released into the cytosol before the endoplasmic vesicles deliver the receptor to the plasma membrane.

Amino acid analysis of FGFR1-4 TM and their predicted conformations provided a number of observations. Only FGFR4 TM domain showed presence of an undisrupted α-helical structure typical for TM domains (Fig. 2). In contrast, the FGFR1 TM is likely to extrude a β-sheet-turn-β structure, which is atypical for membrane spanning TM. Structures of FGFR2 and FGFR3 TM are intermediate between the structures of FGFR1 and FGFR4 with both FGFR2 and FGF3 TM having β-sheets followed by short α-helix. The TM domain in most Group I integral transmembrane proteins form an α-helix. This satisfies the van der Waals requirement for the hydrogen bonding across the helix, therefore, maximizing their membrane association [Voet and Voet, 1995]. In β-sheets, hydrogen bonds form between neighboring polypeptide chains, rather than within the tightly packed helix. The present study indicates that the lack of the typical α helix in the TM of FGFR1 along with short non-polar a.a. chains interrupted by polar a.a. may be critical for the mobilization of FGFR1 from the lipid bilayer and its subsequent trafficking to the nucleus. The chimeric receptor FGFR1/4-EGFP, with the α helical FGFR4 TM displayed decreased cytosol/membrane partition suggesting its stronger association with membranes than the wild type FGFR1–EGFP (Fig. 7A,C). The fact that FGFR1/R4-EGFP was absent from the cytosol argues against the breakage of intracellular organelles as the source of soluble FGFR1 (this was further supported by increased cytosolic content of receptor mutants with increasing TM domain polarity). This shift of FGFR1/4-EGFP towards membrane association was observed both by confocal microscopy imaging of live cells (Fig. 7) and by Western analysis of the microsomal and cytosolic fractions (Fig. 5). Concomitant with this shift FGFR1/4-EGFP displayed diminished intranuclear accumulation. This suggested that cytosolic and nuclear FGFR1 are in equilibrium and release of the receptor from the membrane is the rate-limiting step in FGFR1 trafficking to the nucleus. This mechanism was further supported by the analysis of subcellular distribution of FGFR1(Δ1-3) mutants.

FGFR1(Δ1)-EGFP (V391R) mutation resulted in a small increase in the cytosol/nuclear membrane and cytosol/golgi-ER partitions relative to wild type FGFR1–EGFP. FGFR1(Δ2)-EGFP with two substitutions (V391R) and (C381R) showed further increase in homogenous fluorescence outside golgi-ER and reduced association with membranous structures (Fig. 7A). The chimeric FGFR1/4-EGFP displayed a reduced cytosolic and nuclear receptor accumulation, while increasing the TM domain polarity gradually increased receptor accumulation in the cytosolic-like compartment and the nucleus. These results indicate that soluble FGFR1 enters the nucleus from a soluble receptor pool after being mobilized out of the intracytoplasmic membranes. The increases in the cytosolic receptor concentrations correlate with

its increased receptor accumulation inside the nucleus. The present study indicates that nuclear FGFR1 is in equilibrium with the soluble cytosolic receptor. Nuclear entry of the resident cytosolic FGFR1(SP−)-EGFP, a protein that never associates with membranes, provides further support to the model in which FGFR1 is transported to the nucleus following receptor release from the membrane into the cytosol. This finding is consistent with the report of Reilly and Maher [2001] who found that cytoplasmic FGFR1 is transported to the nucleus by an importin-β dependent process known to carry proteins from the cytosol to the nucleus. Thus, the receptor release from the lipid bilayer is the first step in its nuclear trafficking. Finally, we show that deleting the TM domain did not prevent its nuclear accumulation. Thus the TM does not function as a NLS, but instead allows receptor mobilization out of the membrane into the cytosol. Also, since FGFR1(TM−)-EGFP is likely to accumulate inside the ER lumen because of its localization in the membrane (P150) fraction (Figs. 5 and 6), our results indicate that the nuclear receptor could be derived from ER interior.

Upon arrival of the stop-transfer signal, type 1 membrane proteins anchor themselves firmly in the lipid bilayer by lateral diffusion out of the protein complex that mediates their co-translational insertion [Simon and Blobel, 1991]. Retrograde transport (golgi to cytosol) occurs, and can be viewed as a reversal of integration of membrane proteins into the ER membrane [Matlack et al., 1998; Romisch, 1999]. Therefore, the cytosolic receptor that enters the nucleus through the importin-β mediated transport [Reilly and Maher, 2001] could be derived from golgi-ER membranes. Proteins structurally similar to FGFR1 (i.e., MHC class I molecules [Wiertz et al., 1996], mutant insulin receptor [Immamura et al., 1998], or T cell receptor α [Yang et al., 1998]) are retrieved from the ER membrane into the cytosol. The TM domain of T cell receptor α is divided into short hydrophobic regions [Shin et al., 1993]. These polar disruptions cause the release of T cell receptor α from the ER membrane into cytosol. Similarly, the TM domain of FGFR1 consists of six short continuous runs of non-polar a.a. Their replacement with FGFR4 TM containing a long 12 hydrophobic a.a. run, hindered the receptor accumulation in the cytosol while allowing accumulation in the plasma membrane. The present study suggests that the difference in the TM structure is also critical for the nuclear trafficking of the FGFR1. The retrograde protein transport from ER membrane back to cytosol is coupled to 26S proteasome and the retrieved transmembrane proteins may be degraded in the cytosol [Shin et al., 1993; Immamura et al., 1998]. The increase in cytosolic FGFR1 content observed in lactacystin-treated cells, indicates that ER transmembrane FGFR1 undergoes a similar processing, i.e., release from the ER membrane back into the cytosol where it may be degraded or rapidly transported to the nucleus. Future studies will address the molecular mechanism(s) that move FGFR1 out of the ER membrane into the cytosol and their regulation by stimuli that cause nuclear trafficking of FGFR1. Potential mechanisms could involve dislocation of protein from the membrane by Hsp90 [Immamura et al., 1998]; or CMV U11 gene product [Wiertz et al., 1996] as shown for the insulin receptor and MHC class I molecules, respectively.

The association of FGFR1 and FGF-2 specifically with the nuclear matrix [Stachowiak et al., 1996a,b] suggested that FGFR1 may exert its influence over RNA transcription and processing and DNA replication known to be architecturally organized on the nuclear matrix [Berezney and Coffey, 1977; Zeitlin et al., 1987]. Subsequent studies in our laboratory have revealed that nuclear FGFR1 stimulates histone phosphorylation and transcription of different genes including the tyrosine hydroxylase that encodes the rate-limiting enzyme in catecholamine biosynthesis [Peng et al., 2002], *FGF-2* gene [Peng et al., 2001], and neurofilament gene [Stachowiak et al., 2003] and cyclin A genes (in preparation). Nuclear FGFR1 mediates both the cAMP-induced axonal growth in cultured human neurons [Stachowiak et al., 2003] and BMP-7-induced dendritic growth in rat sympathetic neurons [Horbinski et al., 2002] and glial proliferation [Stachowiak et al., 1997b]. This novel FGFR1 signaling can be initiated by diverse extracellular signals and thus was named integrative nuclear FGFR1 signaling (INFS) [Peng et al., 2001, 2002].

ACKNOWLEDGMENTS

We thank Dr. Pam A. Maher (Scripps Research Institute, La Jolla, CA) for FGFR1 and

FGF-2 antibodies and Mr. Christopher Goulah (SUNY at Buffalo) for assistance with image processing and Mrs. X. Fang, S. Dunham (Graduate Neuroscience Program, SUNY at Buffalo) for help in preparing the manuscript. This study was supported by grants from NSF (IBN-9728923), NIH (HL-49376; R21 NS43621-01) to MKS.

REFERENCES

Baumann CT, Maruvada P, Hager GL, Yen PM. 2001. Nuclear cytoplasmic shuttling by thyroid hormone receptors. J Biol Chem 276:11237–11245.

Berezney R, Coffey DS. 1977. Nuclear matrix: Isolation and characterization of a framework structure from rat liver nuclei. J Cell Biol 73:616–637.

Creighton. Thomas E. 1984. Proteins, structures, and molecular properties. New York: W.H. Freeman and Company. p. 87–90.

Eisenberg D, Schwarz E, Komaromy M, Wall R. 1984. Analysis of membrane surface protein sequences with the hydrophobic moment plot. J Mol Biol 179(1):125–142.

Fenteany G, Standaert RF, Lane WS, Choi S, Corey EJ, Schreiber SL. 1995. Inhibition of proteosome activities and subunit-specific amino-terminal threonine modification by lactacystin. Science 286:726–731.

Florkiewicz RZ, Baird A, Gonzalez AM. 1991. Multiple forms of bFGF: Differential nuclear and cell surface localization. Growth Factors 4:265–275.

Gonzales AM, Berry M, Maher PA, Logan A, Baird A. 1995. A comprehensive analysis of the distribution of FGF-2 and FGFR1 in rat brain. Brain Res 701:201–226.

Guillonneau X, Regnier-Richard F, Laplace O, Jonet L, Bryckaert M, Courtois Y, Mascarelli F. 1998. Fibroblast growth factor (FGF) soluble receptor-1 acts as a natural inhibitor of FGF2 neurotrophic activity during retinal degeneration. Mol Biol Cell 9:2785–2802.

Hanneken A, Maher PA, Baird A. 1995. High affinity immunoreactive FGF receptors in the extracellular matrix of vascular endothelial cells—implications for the modulation of FGF-2. J Cell Biol 128:1221–1228.

Horbinski C, Stachowiak EK, Chandrasekaran V, Miuzukoshi E, Higgins D, Stachowiak MK. 2002. Bone morphogenetic protein-7 stimulates initial dendritic growth in sympathetic neurons through an intracellular fibroblast growth factor signaling pathway. J Neurochem 80:54–63.

Hou J, Kan M, McKeehan K, McBride G, Adams A, McKeehan W. 1991. Fibroblast growth factor receptors from liver vary in three structural domains. Science 251:665–668.

Immamura T, Haruta T, Takata Y, Usui I, Iwata M, Ishibara H, Ishiki M, Ishibashi O, Ueno E, Sasaoka T, Kobayashi M. 1998. Involvement of heat shock protein 90 in degradation of mutant insulin receptors by the proteosome. J Biol Chem 273:11183–11188.

Joy A, Moffett J, Neary K, Shapiro J, Coons S, Mordechai E, Stachowiak EK, Stachowiak MK. 1997. Nuclear accumulation of FGF-2 is associated with proliferation of human astrocytes and glioma cells. Oncogene 14:171–183.

Keegan K, Johnson DE, Williams LT, Hayman MJ. 1991. Isolation of an additional member of the fibroblast growth factor receptor family, FGFR-3. Proc Natl Acad Sci USA 88:1095–1099.

Klimaschewski L, Meisinger C, Grothe C. 1999. Localization and regulation of basic fibroblast growth factor (FGF-2) and FGF receptor-1 in rat superior cervical ganglion after axotomy. J Neurobiol 38:499–506.

Lin SY, Makino K, Xia W, Matin A, Wen Y, Kwong KY, Bourguignon L, Hung MC. 2001. Nuclear localization of EGF receptor and its potential new role as a transcription factor. Nat Cell Biol 3:802–808.

Maher PA. 1996. Nuclear translocation of fibroblast growth factor (FGF) receptors in response to FGF-2. J Cell Biol 134:529–536.

Matlack KES, Mothes W, Rapporport TA. 1998. Protein translocation: Tunnel vision. Cell 92:381–390.

Mayer TU, Braun T, Jentsch S. 1998. Role of proteosome in membrane extraction of a short-lived ER-transmembrane protein. EMBO J 17:3251–3257.

Moffett J, Kratz E, Florkiewicz RZ, Stachowiak MK. 1996. Promoter regions involved in density-dependent regulation of basic fibroblast growth factor gene expression in human astrocytic cells. Proc Natl Acad Sci USA 93:2470–2475.

Ni CY, Murphy MP, Golde TE, Carpenter G. 2001. Gamma-secretase cleavage and nuclear localization of ErbB-4 receptor tyrosine kinase. Science 294(5549): 2179–2181.

Partanen J, Makela TP, Eerola E, Korhonen J, Hirvonen H, Claesson-Welsh L, Alitalo K. 1991. FGFR4, a novel acidic fibroblast growth factor receptor with a distinct expression pattern. EMBO J 10:1347–1354.

Peng Hu, Moffett J, Myers J, Fang X, Stachowiak EK, Maher PA, Kratz E, Hines J, Fluharty SJ, Mizukoshi E, Bloom DC, Stachowiak MK. 2001. A novel nuclear signaling pathway mediates activation of the *FGF-2* gene by AT1 and AT2 angiotensin II receptors. Mol Biol Cell 12:449–462.

Peng Hu, Myers J, Fang X, Stachowiak EK, Maher PA, Martins GG, Popescu G, Berezney R, Stachowiak MK. 2002. Integrative nuclear FGFr1 signaling (INFS) pathway mediates activation of the tyrosine hydroxylase gene by angiotensin II, depolarization, and protein kinase C. J Neurochem 81:506–524.

Plotnikov AN, Schlessinger J, Hubbard SR, Mohammadi M. 1999. Structural basis for FGF receptor dimerization and activation. Cell 98:641–650.

Reilly JF, Maher PA. 2001. Importin-β mediated nuclear import of fibroblast growth factor receptor: Role in cell proliferation. J Cell Biol 152:1307–1312.

Renko M, Quatro N, Morimoto T, Rifkin DB. 1990. Nuclear and cytoplasmic localization of different basic fibroblast growth factor species. J Cell Physiol 144: 108–114.

Reyes VE, Philips L, Humphreys RE, Lew RA. 1989. Prediction of protein helices with a derivative of the strip-of-helix hydrophobicity algorithm. J Biol Chem 264: 12854–12858.

Romisch K. 1999. Surfing the Sec61 channel: Bidirectional protein translocation across the ER membrane. J Cell Sci 112:4185–4191.

Shiang R, Thompson LM, Zhu YZ, Church DM, Fielder TJ, Bocian M, Winokur ST, Wasmuth JJ. 1994. Mutations in the transmembrane domain of FGFR3 cause the most common genetic form of dwarfism, achondroplasia. Cell 78:335–342.

Shin J, Lee S, Strominger JL. 1993. Translocation of TCRα chains into the lumen of the endoplasmic reticulum and their degradation. Science 259:1901–1904.

Simon SM, Blobel G. 1991. A protein-conducting channel in the endoplasmic reticulum. Cell 65:371–380.

Stachowiak EK, Fag X, Myers J, Dunham S, Stachowiak MK. 2003. cAMP-iduced differentiation of human neuronal progenitor cells is mediated by nuclear FGF receptor-1. J Neurochem in press.

Stachowiak MK, Moffet J, Joy A, Puchacz EK, Florkiewicz R, Stachowiak EK. 1994. Regulation of *bFGF* gene expression and subcellular distribution of bFGF protein in adrenal medullary cells. J Cell Biol 127:203–223.

Stachowiak MK, Maher PA, Joy A, Mordechai E, Stachowiak MK. 1996a. Nuclear accumulation of fibroblast growth factor receptors is regulated by multiple signals in adrenal medullary cells. Mol Biol Cell 7:1299–1317.

Stachowiak MK, Maher PA, Joy A, Mordechai E, Stachowiak EK. 1996b. Nuclear localization of functional FGF receptor 1 in human astrocytes suggests a novel mechanism for growth factor action. Mol Brain Res 38:161–165.

Stachowiak EK, Maher PA, Tucholski J, Mordechai E, Joy A, Moffett J, Coons S, Stachowiak MK. 1997a. Nuclear accumulation of fibroblast growth factor receptors in human glial cells-association with cell proliferation. Oncogene 14:2201–2211.

Stachowiak MK, Moffett J, Maher PA, Tucholski J, Stachowiak EK. 1997b. Growth factor regulation of cell growth and proliferation in the nervous system. A new intracrine nuclear mechanism. Mol Neurobiol 15: 1–27.

Stroud RM, Walter P. 1999. Signal sequence recognition and protein targeting. Curr Opin Struct Biol 9:754–759.

Szebeneyi G, Fallon JF. 1999. Fibroblast growth factors as multifunctional signaling factors. Int Rev Cytol 185:45–106.

Viswanadhan VH, Denckla B, Weinstein JN. 1991. New joint prediction algorithm (Q7-JASEP) improves the prediction of protein secondary structure. Biochemistry 30(46):11164–11172.

Voet Donald, Voet Judith. 1995. Biochemistry. 2nd edition. New York: John Wiley & Sons, Inc.

Walter P, Johnson AE. 1994. Signal sequence recognition and protein targeting to the endoplasmic reticulum membrane. Annu Rev Cell Biol 10:87–119.

Wiertz EJHJ, Jones TR, Sun L, Bogyo M, Geuze HJ, Ploegh HL. 1996. The human cytomegalovirus US11 gene product dislocates MHC class I heavy chains from the endoplasmic reticulum to the cytosol. Cell 84:769–779.

Yang BM, Omura S, Bonifacino JS, Weissman AM. 1998. Novel aspects of degradation of T cell receptor subunits from the endoplasmic reticulum (ER) in T cells: Importance of oligosaccharide processing, ubiquitination, and proteoasome-dependent removal from ER membranes. J Exp Med 187:835–846.

Zeitlin S, Parent A, Silverstein S, Efstratiadis A. 1987. Pre-mRNA splicing and the nuclear matrix. Mol Cell Biol 7(1):111–120.